Imidazolyl Carboxylic Acids As Mechanistic Probes of Flavocytochrome P-450 BM3[†]

M. A. Noble,[§] L. Quaroni,[‡] George D. Chumanov,[‡] K. L. Turner,[§] S. K. Chapman,[§] R. P. Hanzlik,[||] and A. W. Munro*,[§]

Department of Chemistry, The University of Edinburgh, The King's Buildings, West Mains Road, Edinburgh EH9 3JJ, U.K., Department of Chemistry, Iowa State University, Ames, Iowa 50011, and Department of Medicinal Chemistry, University of Kansas, Lawrence, Kansas 66045

Received February 26, 1998; Revised Manuscript Received July 20, 1998

ABSTRACT: ω-Imidazolyl carboxylic acids (C10−C12) have been used as probes of the active site and catalytic mechanism of the fatty acid hydroxylase P-450 BM3 from *Bacillus megaterium*. These compounds are the most potent inhibitors of P-450 BM3 yet reported. All are mixed inhibitors, increasing the K_m and decreasing the k_{cat} for laurate oxidation. All ligate the P-450 BM3 ferric heme iron, inducing a type II shift in the Soret absorbance band from 419 to 424 nm. Binding to the ferrous form is much weaker. 10-(Imidazolyl)decanoic acid was the best inhibitor ($K_{ic} = 0.9$ μM, $K_{iu} = 5.7$ μM), while 12-(imidazolyl)-dodecanoic acid ($K_{ic} = 1.35$ μM, $K_{iu} = 6.9$ μM) was superior to 11-(imidazolyl)undecanoic acid ($K_{ic} = 7.5$ μM, $K_{iu} = 16$ μM). Dissociation constants for binding to oxidized P-450 BM3 heme iron were determined spectrophotometrically as 8 μM (C12 azole) and 27 μM (C11 azole). The binding of 10-(imidazolyl)decanoic acid was too tight for an absolute K_d to be determined spectrophotometrically, but this value is <0.2 μM. The binding of different fatty acids to the enzyme was found to have distinct effects on the K_d for the azoles. Laurate induced tighter binding (K_d for the C12 azole lowered to 4.7 μM), while arachidonate weakened the affinity (K_d increased to 23 μM). Arachidonate diminished the affinity for the C10 azole sufficiently that a K_d could be determined by spectrophotometric titration (11 μM). Affinity for the C12 azole was decreased in active-site-mutants R47G (R47 tethers the fatty acid carboxylate group) and F87Y but increased in mutant F87G—indicating an important role for this residue in determining heme accessibility. The C10 azole binds much more weakly to the spin-state-insensitive F87Y (32.2 μM), suggesting that the inhibitors may bind preferentially to different conformers of P-450 BM3. $NADP^+$ binding in the reductase also tightened affinity of these inhibitors for P-450 BM3 (K_d for the C12 azole decreased to 2.7 μM), but this effect was not observed for FMN-deficient mutant W574D, suggesting that the interdomain effect of $NADP^+$ on inhibitor binding was mediated via flavin mononucleotide. Resonance Raman spectroscopy indicates that the inhibitors form low-spin complexes with P-450 BM3 and that their binding induces movements of the heme vinyls relative to the ring.

The involvement of the cytochromes P-450[1] in a vast array of cellular processes is well-known, as is their ability to oxidize numerous drugs and organic xenobiotics, thus facilitating their excretion from cells or, in the case of microbes, permitting their use as energy sources (*1*, *2*). Their substrate range is enormous, extending from simple molecules such as acetone through to complex polycyclic compounds. Eukaryotic P-450s are usually membrane-bound and interact with membranous redox partners. Bacterial forms (and their redox partners) are generally soluble. The soluble bacterial forms have proved the most experimentally tractable systems and X-ray crystal structures have now been obtained from six bacterial forms (*2*−*4*). The most extensively studied of these are the camphor hydroxylase P-450cam from *Pseudomonas putida* and the fatty acid hydroxylase P-450 BM3 from *Bacillus megaterium* (*2*). In recent years, the P-450 BM3 system has been the subject of intense scrutiny, with the realization that it operates an electron-transfer system similar to that used by mammalian drug-metabolizing forms (P-450 and diflavin P-450 reductase) and also because the heme domain of P-450 BM3 is fused to its diflavin reductase in a single polypeptide, an arrangement similar to that of the nitric oxide synthases (*5*). The atomic structures of the substrate-free and substrate- (palmitoleate-) bound forms of the heme domain of P-450 BM3 have been determined (*6*,

[†] We thank the Royal Society of Edinburgh for the awards of a Caledonian Research Foundation Fellowship (A.W.M.) and SOEID Support Fellowship (S.K.C.) and the Leverhulme Trust (postdoctoral assistantship to M.A.N.). We also thank the BBSRC for their support of these studies (studentship to K.L.T.). L.Q. and G.D.C. are supported by the NIH (Grant NIH-GM48000).

* Author to whom correspondence should be addressed: Tel +44 131 650 4753; Fax +44 131 650 4760; E-mail Andrew.Munro@ed.ac.uk.

[§] The University of Edinburgh.

[‡] Iowa State University.

[||] University of Kansas.

[1] Abbreviations: Abs, absorbance; FAD, flavin adenine dinucleotide; FMN, flavin mononucleotide; ImC10, 10-(imidazolyl)decanoic acid; ImC11, 11-(imidazolyl)undecanoic acid; ImC12, 12-(imidazolyl)-dodecanoic acid; IPTG, isopropyl β-D-thiogalactopyranoside; MOPS, 3-(*N*-morpholino)propanesulfonic acid; $NADP^+$/H, nicotinamide adenine dinucleotide phosphate (oxidized/reduced); P-450, cytochrome P-450 monooxygenase; PMSF, phenylmethanesulfonyl fluoride.

10.1021/bi980462d CCC: $15.00
Published on Web 10/22/1998

7). These structures have provided the basis for rational mutagenesis aimed at the determination of the roles of key active-site residues. Such studies have identified determinants of heme binding and spin-state control (W96; *8*), of regiospecificity of substrate oxidation (F87; *9*, *10*), and of fatty acid ligation in the active site (R47, *11*).

The study of P-450 inhibitors and their mechanisms of action is a major focus of interest in the pharmaceutical industry for the rational design of fungicides and insecticides and has major medical implications (e.g., in human drug metabolism and steroid synthesis pathways). Substrate-like compounds containing an imidazole functionality (capable of ligating the heme iron) have found most widespread use. For instance, steroid-derived azole antifungal agents provide the basis of a multimillion dollar industry; with their target as the 14α-sterol demethylase P-450 required for the synthesis of the important membrane lipid ergosterol (*12*). Analysis of the action of inhibitors of the P-450s and the mechanisms by which they function has been important in elucidating important features of the structures of active sites of various isoforms and of the catalytic processes employed (e.g., refs *13* and *14*).

We have examined the binding characteristics and inhibition kinetics of P-450 BM3 with imidazolyl carboxylic acids, potential heme-coordinating mimics of the natural fatty acid substrates of P-450 BM3. Our results indicate these compounds are the most potent inhibitors of P-450 BM3 yet reported. The data also provide evidence for interdomain communication between the heme (P-450) and diflavin (reductase) domains of this model flavocytochrome and indicate that the binding of either pyridine nucleotide or fatty acid substrate or mutation at key catalytic residues can affect dramatically the binding of the inhibitors to the P-450 BM3 active site.

EXPERIMENTAL PROCEDURES

Materials. All P-450 BM3 substrates and other reagents were purchased from Sigma and were of the highest possible grade. The fatty acids used were sodium laurate and arachidonic acid. Stock solutions of laurate (50 mM) and arachidonic acid (33 mM) were made up in 1:1 (v/v) methanol/ethanol. NADPH (20 mM) was prepared in ice-cold assay buffer [20 mM MOPS (pH 7.4) + 100 mM KCl]. 10-(Imidazolyl)decanoic acid, 11-(imidazolyl)undecanoic acid, and 12-(imidazolyl)dodecanoic acid were synthesized and purified as previously described (*15*).

Escherichia coli Strains and Plasmid Vectors. E. coli strain TG1 [*sup*E *hsd*Δ5 *thi* Δ(*lac*−*pro*AB) F′ (*tra*D36 *pro*AB$^+$ *lac*I^q *lac*ZΔM15)] was used for all cloning work and for overexpression of intact P-450 BM3 and its heme domain. The preparation of the constructs for the overexpression of intact P-450 BM3 (plasmid pBM25) and the heme domain (plasmid pBM20) has been presented in previous publications (*16*, *17*). Plasmid clones encoding the active-site mutants R47G, F87G, and F87Y of P-450 BM3 were obtained from Dr. David Mullin and Professor William Alworth (Department of Chemistry, Tulane University, New Orleans, LA) and overexpressed under a T7 promoter system from plasmid vector pTZ18U in strain BL21 (DE3) [*hsd*S *gal* (λc I*ts*857 *ind*1 Sam7 *nin*5 *lac*UV5−T7 gene 1)]. The clone encoding FMN-deficient mutant W574D in plasmid pBluescript (Stratagene) was obtained from Professor Armand Fulco (Department of Chemistry, UCLA) (*18*) and expressed from strain TG1 in identical fashion to the wild-type clone (*17*).

Enzyme Preparations. Intact cytochrome P-450 BM3 and its heme domain were purified as described previously (*16*, *17*). Protein was purified from *E. coli* transformants TG1/pBM25 and TG1/pBM20 by growth of the transformant cultures (2−5 L in LB medium, 37 °C, 250 rpm) for 6−12 h after induction at $OD_{600} = 1$ with 250 μg/mL IPTG. All mutants of flavocytochrome P-450 BM3 were purified exactly as described for the wild-type enzyme (*17*). Expression of the W574D mutant was from TG1 transformants as described for the wild-type P-450 BM3. Expression of mutants R47G, F87Y, and F87G was from BL21 (DE3) transformants. Cells (2−5 L in LB medium) were collected 5 h post-induction with 500 μg/mL IPTG. A final gel-filtration step (Sephacryl S-200HR) was used to remove minor contaminating protein species. PMSF (1 mM) and leupeptin (1 mM) were added to all buffers to minimize proteolysis. All proteins were stored at −20 °C after dialyzing twice successively into 500-fold volumes of buffer A [50 mM Tris·HCl (pH 7.2) and 1 mM EDTA] containing 50% glycerol and protease inhibitors and were used within 1 month of manufacture.

Spectrophotometric and Kinetic Characterization. Aerobic UV−visible spectra were collected with a Shimadzu 2101 spectrophotometer. Spectrophotometric and rate measurements were performed in quartz cells of 1 cm path length. The concentration of heme protein used in titrations with the inhibitors was 3−8 μM. Inhibitors were added in small (0.1−0.4 μL) aliquots (<5 μL total addition) from concentrated stocks (25−60 mM) prepared in DMSO:methanol (1:1 v/v). All titrations were performed at 30 °C in assay buffer. In attempts to determine K_d values for the binding of the ImC10 inhibitor to P-450 BM3 and mutant forms, heme protein concentrations of 0.2−0.4 μM were used in titrations performed in a 5 cm path length cell with a Unicam ATI UV2 spectrophotometer. Other conditions were as described above. For spectrophotometric titrations of substrates and inhibitors, dilution effects were accounted for by multiplication of the spectra by the appropriate factor. Difference spectra for each titration set were generated by successive subtractions of the spectrum of the inhibitor-free enzyme from the spectrum after each addition of inhibitor (after appropriate corrections were made). Maximal absorbance changes were computed by subtraction of the absorbance value at the trough from that at the peak of each difference spectrum (using the same λ values in each titration). K_d values were derived by fitting the resulting absorbance difference values (A) plotted against the inhibitor concentration values ([I]) to a hyperbolic function: $A = A_{max}[I]/(K_d + [I])$.

Anaerobic titrations of reduced enzyme were conducted within a Belle Technology glovebox under a nitrogen atmosphere, with oxygen maintained at less than 5 ppm. All samples were bubbled with oxygen-free nitrogen (30 min) prior to transferring to the glovebox. Degassed enzyme samples were passed through an anaerobic Sephadex G25 column (1 × 20 cm) (Sigma) immediately on admission to the glovebox, thereby removing all traces of oxygen. The column was equilibrated and enzyme was eluted with assay

buffer. Spectra were recorded on a Shimadzu 1201 UV−vis spectrophotometer (typically between 250 and 800 nm) contained within the anaerobic environment. Reduced enzyme samples were generated anaerobically by addition of the minimum quantity of sodium dithionite solution (50 mM stock in degassed buffer) required to cause fusion of the heme α and β bands and a shift of the Soret band to 412 nm, features typical of the reduced P-450 form (*19*). All data manipulations and nonlinear least-squares curve-fitting of titration and kinetic data were conducted with Origin (Microcal).

Measurements of lauric acid oxidation rates were made at 30 °C using 20−50 nM P-450 BM3 and 200 μM NADPH in the assay buffer as described previously (*16*, *17*, *20*). Initial rates of fatty acid (sodium laurate) monooxygenation were measured by following the oxidation of NADPH at 340 nm (6210 M^{-1} cm^{-1}) over the first 10−15 s at 30 °C in assay buffer, with the enzyme concentration between 5 and 10 nM and NADPH at saturating levels (200 μM). The reversible inhibition characteristics of ImC10, ImC11, and ImC12 were evaluated by their effect on the K_m and k_{cat} for laurate hydroxylation. The K_i values were determined from the apparent K_m and k_{cat} values obtained from repetitions of the Michaelis curve for laurate hydroxylation at 3−4 different, fixed inhibitor concentrations (0.4−10 μM).

Spectroscopic Characterization. Resonance Raman spectra of the P-450 BM3 heme domain were recorded with a Coherent Innova 100 Krypton ion laser as the source of 413.1 nm radiation. Power at the sample was kept at 15−20 mW. Scattered radiation was collected at 180°, analyzed by a Spex 1877 triple monochromator, and measured by a Princeton Instruments 1152E LN/CCD detector. The heme domain was 1.6×10^{-5} M in 0.1 M sodium phosphate buffer at pH 7.4. ImC10 and ImC12 inhibitors were added from concentrated DMSO/MeOH stocks (as described above) to give a final concentration of 345 μM for ImC10 and 191 μM for the ImC12 derivative. The same quantity of solvent was added for both measurements. Far UV circular dichroism (CD) spectra (between 190 and 260 nm) were recorded at 20 °C in a Jasco J600 spectropolarimeter for wild-type P-450 BM3 (3 μM) ± 100 μM ImC10 or ImC12.

RESULTS

Kinetic Studies. The ImC10 and ImC12 compounds proved to be very potent inhibitors of fatty acid monooxygenation by P-450 BM3. ImC11 was less efficient. The relative potency of the inhibitors was evaluated by their effect on the Michaelis parameters for laurate hydroxylation. A preliminary comparison was performed at inhibitor concentrations of 3.2 μM and a fixed laurate concentration of 400 μM. The rates of laurate hydroxylation were determined (in moles $minute^{-1}$ $mole^{-1}$) as 672 ± 19 (ImC11), 316 ± 11 (ImC12), and 137 ± 9 (ImC10) compared with 1018 ± 22 (uninhibited). ImC10 is the most efficient inhibitor.

An increase in K_m and a decrease in k_{cat} were observed for the laurate-dependent oxidation of NADPH with all three inhibitors. These are characteristic of mixed inhibition, whereby the inhibitor can bind to both free enzyme (E) and the enzyme−fatty acid (ES) complex in the Michaelis−Menten mechanism (Scheme 1). To determine the relative

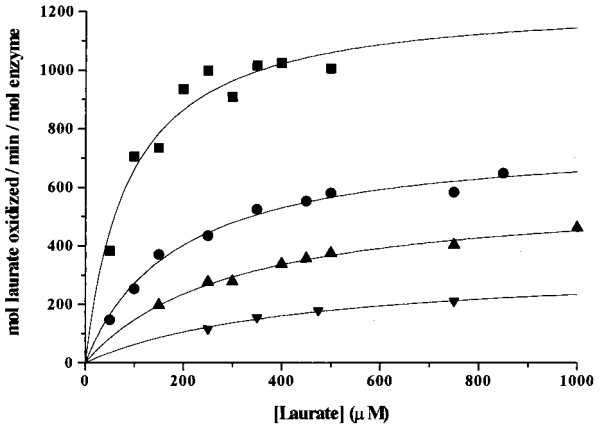

FIGURE 1: Michaelis−Menten curves for the oxidation of sodium laurate by P-450 BM3, uninhibited and in the presence of 4.2, 8.4, and 16.8 μM ImC12. Reactions were performed at 30 °C as described in the Experimental Procedures section. The decrease in apparent K_m [$K_{m(app)}$] and apparent k_{cat} [$k_{cat(app)}$] is typical of the action of a mixed inhibitor. (■) No inhibitor, $K_m = 89 \pm 18$ μM, $k_{cat} = 1252 \pm 70$ min^{-1}; (●) 4.2 μM ImC12, $K_{m(app)} = 188 \pm 20$ μM, $k_{cat(app)} = 780 \pm 28$ min^{-1}; (▲) 8.4 μM ImC12, $K_{m(app)} = 306 \pm 29$ μM, $k_{cat(app)} = 593 \pm 22$ min^{-1}; (▼) 16.8 μM ImC12, $K_{m(app)} = 453 \pm 77$ μM, $k_{cat(app)} = 342 \pm 28$ min^{-1}. Similar phenomena were observed for the ImC10 and ImC11 inhibitors.

Scheme 1: Characteristics of Action of a Mixed Inhibitor (I) Binding to both Free Enzyme (E) and Enzyme−Substrate Complex (ES) To Form EI and ESI with Dissociation Constants K_{ic} and K_{iu}, Respectively (*21*)

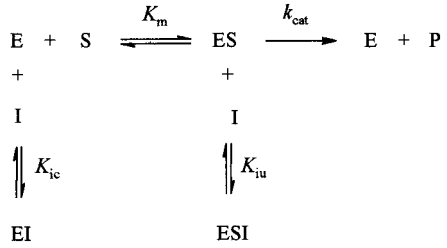

dissociation constants for E and ES (K_{ic} and K_{iu}, respectively) the following equations for mixed inhibition were used:

$$k_{cat(app)} = \frac{k_{cat}}{1 + [I]/K_{iu}} \quad (1)$$

$$K_{m(app)} = \frac{K_m(1 + [I]/K_{ic})}{1 + [I]/K_{iu}} \quad (2)$$

$k_{cat(app)}$ and $K_{m(app)}$ represent the apparent k_{cat} and K_m at each of the different concentrations of inhibitor used. Values of 1.35 ± 0.36 μM and 6.94 ± 1.26 μM, respectively, were calculated for K_{ic} (dissociation constant for the free enzyme) and K_{iu} (dissociation constant for the ES complex) (*21*) for ImC12 (Figure 1). The analogous values for ImC11 were 7.5 ± 2.7 μM and 16.2 ± 3.7 μM, and for ImC10 they were 0.87 ± 0.39 μM and 5.7 ± 2.73 μM.

Spectrophotometric Titrations: (A) Substrate-Free P-450 BM3. Spectrophotometric titrations of oxidized flavocytochrome P-450 BM3 (2−4 μM) were performed at 30 °C in assay buffer, monitoring the absorbance change between 800 and 300 nm upon addition of the imidazoles (which have no absorbance in this region). All inhibitors induced a type II absorbance shift of the heme Soret band, indicating ligation of the azole group to the heme iron. A red shift of 5 nm

Table 1: Visible Spectroscopic Properties of Wild-Type Flavocytochrome P-450 BM3 in Its Oxidized/Ligand-Free Form, Substrate-Saturated (High-Spin) Form, and in the Presence of Saturating Concentrations of the Alkyl Imidazole Inhibitors

	absorbance maxima (nm)				
	absolute spectra			difference spectra[b]	
enzyme state	Soret	β	α	peak	trough
substrate-free	419	534	567.5		
Ara-bound	391	shoulder $\sim$ 542		389	420.5
Imid-bound	424	540	571	432	410
Imid/Ara-bound	424	540	571	425	391

[a] Ara = arachidonic acid; Imid = ImC10, ImC11, and ImC12, all giving identical spectral shifts. [b] Difference spectra were generated by subtraction of the spectrum of the substrate-free oxidized form from that of the arachidonic acid-bound form (Ara-bound) or the alkyl imidazole-bound form (Imid-bound); or by the subtraction of the spectrum of the arachidonate-bound form from that of the same complex saturated with an alkyl imidazole (Ara/Imid-bound). Titrations with substrate/inhibitors were performed as described in the Experimental Procedures section.

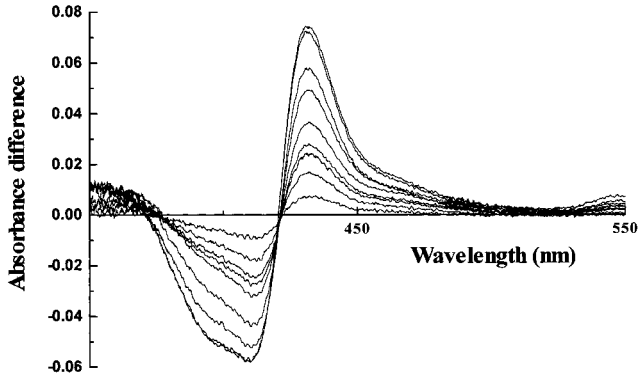

FIGURE 2: Difference spectra for the titration of 5 μM oxidized substrate-free wild-type P-450 BM3 with the ImC10 inhibitor. Difference spectra were generated by subtraction of the spectrum of the azole-free form from each successive spectrum generated by ImC10 additions. The traces showing increasing deviation from the baseline correspond to addition of 9.1, 18.3, 27.4, 36.5, 45.6, 63.8, 82.0, 119, and 228 μM ImC10, respectively. Titrations were performed as described in the Experimental Procedures section.

from 419 to 424 nm was observed on saturation of the P-450, with smaller changes in the longer wavelength region where the heme α and β bands are located (530−580 nm) (Table 1). Isosbestic points for the oxidized inhibitor-free and inhibitor-bound forms are located at approximately 422 and 559 nm. Alterations in the spectra induced by the inhibitors are more clearly distinguished in the difference spectra (Figure 2).

Dissociation constants (K_ds) were determined by fitting the maximal spectral absorbance difference observed vs the concentration of inhibitor to a rectangular hyperbola. For both ImC12 and ImC11, this procedure resulted in good fits of the data points to the function. The K_d determined for ImC12 is lower (8 μM) than that obtained for ImC11 (27 μM) (Table 2). This finding was not unexpected in view of the known preference for longer chain fatty acids as substrates for P-450 BM3. For saturated fatty acids, activity is maximal toward C16 (palmitic acid, K_m approximately 2 μM), with C12 oxidized more slowly and bound rather less tightly (lauric acid, K_m approximately 100 μM) (*8*). While the imidazolyl carboxylic acids have relatively short carbon chain length (C10−C12), the imidazole ring adds considerable size to the

Table 2: Dissociation Constants for the Binding of the Imidazolyl Carboxylic Acid Inhibitors to Wild-type Flavocytochrome P-450 BM3 in Its Oxidized, Substrate-Bound, $NADP^+$-Bound, and $NADP^+$/Substrate-Bound Forms[a]

	inhibitor K_d (μM)		
enzyme form[b]	ImC10	ImC11	ImC12
ox.-free	$\leq$0.2	27.2 $\pm$ 1.4	8.0 $\pm$ 0.2
ox.-Laur	$\leq$0.2	10.5 $\pm$ 0.4	4.7 $\pm$ 0.6
ox.-Ara	10.7 $\pm$ 0.3	348 $\pm$ 28	23.3 $\pm$ 0.4
ox.-$NADP^+$	$\leq$0.2	21.0 $\pm$ 1.4	2.7 $\pm$ 0.1
ox.-Laur/$NADP^+$	$\leq$0.2	11.3 $\pm$ 0.6	3.4 $\pm$ 0.4
ox.-Ara/$NADP^+$	13.5 $\pm$ 0.7	133 $\pm$ 9	22.0 $\pm$ 0.5

[a] Titrations were performed as described in the Experimental Procedures section. [b] Ox. = oxidized; Laur = sodium laurate; Ara = arachidonic acid.

inhibitors. However, at concentrations of protein (ca. 4 μM) convenient for spectrophotometric determination of the K_d, the data for the ImC10 titrations are not described by a hyperbolic function. Rather, there is a linear increase in the heme absorbance difference induced with increasing [ImC10], which sharply plateaus to reach an absolute value. Experiments in which spectra were recorded during dilution of enzyme/ImC10 complexes with the assay buffer showed that the titration curve followed the same nonhyperbolic pattern during the dilution, indicating that binding of ImC10 was reversible (not shown). Such behavior is easily explained if the K_d for the inhibitor binding is significantly lower than the enzyme concentration. To demonstrate that very tight binding of ImC10 was responsible for the unusual titration curves observed, titrations were repeated with a longer path length (5 cm) quartz cell at a much lower enzyme concentration (0.2 μM). Again, the initially linear but abruptly breaking titration curve was produced. However, the curve was seen to plateau at a much lower concentration of ImC10, suggesting that very tight binding was indeed the explanation. Further titrations of ImC10 in the presence of fatty acid substrates (discussed below) confirmed this to be the case.

Anaerobic titrations with reduced P-450 BM3 indicated that all the inhibitors could ligate to the ferrous heme, albeit more weakly than to the ferric form, inducing a red (type II) shift of the Soret absorbance band to approximately 424 nm. The K_d values were 45.94 $\pm$ 3.5 μM (ImC10), 34.38 $\pm$ 6.42 μM (ImC11), and 26.4 $\pm$ 9.6 μM (ImC12).

(B) Fatty Acid-Bound P-450 BM3. The observation of mixed inhibition from the kinetic data indicated that the inhibitors might retain high affinity for the substrate-bound forms of P-450 BM3. To examine this possibility, titrations with all the imidazoles were also performed with substrate (arachidonic acid and sodium laurate) saturated P-450 BM3, using 70 μM arachidonic acid (K_d 1.5 μM) or 500 μM sodium laurate (K_d 100 μM) to saturate 3 μM P-450. This quantity of arachidonic acid, the best substrate for P-450 BM3 yet reported, induces spectral shifts typical of the conversion to high-spin heme iron (Table 1) and results in >90% conversion to the high-spin form (Soret absorbance maximum shifts from 419 to 390 nm) (*19*). By contrast, saturation with sodium laurate converts the protein to only approximately 30% high-spin heme iron (*8, 19*).

It was found that saturating sodium laurate enhanced the binding of the ImC12 and ImC11 inhibitors to P-450 BM3. The K_ds were lowered to 4.7 μM (from 8.0 μM) for ImC12

and to 10.5 μM (from 27.2 μM) for ImC11. By contrast, saturating concentrations of arachidonic acid caused large increases in the K_d values for the binding of ImC12 (23.3 μM) and ImC11 (348 μM). The binding of ImC10 to laurate-saturated P-450 BM3 remained too tight for a K_d to be determined by spectrophotometric titration, even when the experiment was performed at low enzyme concentration (0.2 μM) in the 5 cm path length cell. However, the ImC10 titration of 0.2 μM P-450 BM3 saturated with arachidonate (performed in the 5 cm cell) yielded a good rectangular hyperbola characterized with a K_d of 11 μM. Clearly, arachidonate also weakens significantly the affinity of ImC10 for P-450 BM3. In the presence of arachidonate, the K_d for ImC12 binding to P-450 BM3 increases 3-fold (from 8 to 23 μM) while that for ImC11 increases approximately 15-fold (from 27 to 348 μM) (Table 2). Thus, in the presence of arachidonate, affinity of P-450 BM3 is weakened for all imidazolyl fatty acids by a large enough factor to allow measurement of a K_d by conventional spectrophotometric titration. For substrate-free P-450 BM3, binding of ImC10 is very tight and the K_d is very low; $\leq$0.2 μM, the concentration of enzyme used in the titrations.

Anaerobic additions of ImC10−ImC12 to sodium dithionite-reduced, substrate (laurate, arachidonate)-bound forms of P-450 BM3 did not result in any absorbance changes of the heme bands. This indicates the inhibitors are unable to ligate to the ferrous, substrate-bound form of P-450 BM3.

(C) NADP$^+$-Bound P-450 BM3. In Scheme 1 shown above, it appears that the binding of inhibitors to the free enzyme (characterized with dissociation constant K_{ic} from kinetic measurements) is analogous to the K_d determined spectrophotometrically. However, the discrepancy between K_{ic} values and the K_d values calculated for ImC11 and ImC12 ($K_{ic} < K_d$ in all cases; e.g., for ImC12, $K_{ic} = 1.35$ μM and $K_d = 8.0$ μM) suggested that other factors may influence affinity for the inhibitors. The only component absent in Scheme 1 is the pyridine dinucleotide coenzyme (NADP$^+$/H), which binds to the reductase domain of P-450 BM3. In view of recent fluorescence data (*22*), which indicate that interdomain effects occur on fatty acid binding to the enzyme, we decided to investigate the influence of bound NADP$^+$ on the affinities for the inhibitors as a possible reason for the differences in K_{ic} vs K_d.

Spectrophotometric titrations of P-450 BM3 saturated with 200 μM NADP$^+$ ($K_d \leq 2$ μM) were performed with each of the three inhibitors. In all cases, the K_d values were decreased by binding of NADP$^+$. For ImC12, the K_d was lowered from 8.0 to 2.7 μM, and for ImC11, from 27.2 to 21.0 μM (Table 2). Again, as expected, the form of the titration curve for ImC10 with NADP$^+$-saturated P-450 BM3 indicated very tight binding. A K_d could not be determined spectrophotometrically. Evidently, binding of ImC10 to NADP$^+$-bound P-450 BM3 is at least as tight as to the NADP$^+$-free form.

(D) Flavocytochrome P-450 BM3 Heme Domain. K_d measurements for inhibitor binding to the heme domain of P-450 BM3 (*16*) were made to assess the influence of removing the diflavin reductase on the affinity for the ImC10 and ImC12 inhibitors. For substrate-free heme domain, the K_d for ImC12 was slightly increased by comparison with the intact P-450 BM3 (12.1 vs 8.0 μM), whereas the K_d for ImC11 was very similar (27.1 vs 27.2 μM). The binding of ImC10 to the heme domain remained very tight ($K_d < 0.2$ μM). However, laurate-saturated heme domain gave a K_d of 8.1 μM for ImC12 (vs 4.7 μM for intact P-450 BM3) and arachidonate-saturated heme domain gave K_ds of 17.1 μM for ImC10 (vs 10.7 μM) and 149 μM for ImC12 (vs 23.3 μM). There is a broadly lower affinity of the inhibitors (certainly for ImC10 and ImC12) for the heme domain vs intact P-450 BM3. This pattern is reminiscent of the comparative K_d values with true fatty acid substrates. The distinct effects of laurate and arachidonate binding to the heme domain on its affinities for ImC10 and ImC12 are similar to those observed for the intact P-450 BM3. As with intact P-450 BM3, arachidonate binding weakens ImC10 affinity for the heme domain sufficiently that a K_d (= 17.1 μM) can be measured in the 5 cm cell (Tables 2 and 3).

Table 3: Dissociation Constants for the Binding of the ImC10 and ImC12 Inhibitors to Site-directed Mutants of Flavocytochrome P-450 BM3 in Their Oxidized Forms and to the Substrate-Free and Substrate-Bound Forms of the Heme Domain (P-450) of Wild-type Flavocytochrome P-450 BM3[a]

	inhibitor K_d (μM)	
enzyme form	ImC10*	ImC12
R47G	4.3 ± 0.4	42.2 ± 1.0
F87G	≤0.2	5.3 ± 0.1
F87Y	32.2 ± 1.4	24.3 ± 2.6
W574D	≤0.2	7.7 ± 0.5
W574/NADP$^+$	≤0.2	8.5 ± 0.3
P-450	≤0.2	12.1 ± 1.0
P-450-Laur	≤0.2	8.1 ± 0.3
P-450-Ara	17.1 ± 1.0	149 ± 3

[a] Titrations were performed as described in the Experimental Procedures section. [b] Laur = sodium laurate; Ara = arachidonic acid.

(E) Mutant Enzymes. To investigate the possibility that mutation at key catalytic residues might affect the affinity and binding characteristics of the ImC10 and ImC12 inhibitors, dissociation constants were determined for mutants R47G, F87G, F87Y, and W574D (Table 3). Residues R47, F87, and W574 have roles critical to fatty acid carboxylate tethering to the enzyme (R47; *10*), control of regiospecificity of substrate oxidation (F87; *9*, *11*), and binding of the FMN cofactor (W574; *17*, *18*).

In R47G, ImC12 affinity was decreased relative to the wild-type enzyme (42.2 vs 8.0 μM). This increased K_d would be expected if interaction between the positively charged guanidinium group and the negatively charged carboxylate of the ImC12 is important to the binding of the azole, as seems to be the case for fatty acid substrates (*10*). ImC10 binding curves remained nonhyperbolic for R47G, measured at an enzyme concentration of 4 μM in a 1 cm path length cell. However, at lower R47G concentration (0.2 μM) in a 5 cm cell, the ImC10 titration data accurately fit a rectangular hyperbola and a K_d value of 4.3 μM was determined (Table 3).

Mutant F87G has increased affinity for ImC12 ($K_d = 5.3$ μM), whereas the affinity of F87Y for ImC12 is considerably decreased ($K_d = 24.3$ μM). Residue F87 undergoes a conformational change on substrate association (*7*). The phenyl ring of F87 lies just above and parallel to the heme in the oxidized substrate-free form and rotates to a perpendicular orientation when substrate binds (*6*). Removal of the aromatic side chain in F87G may improve access to the heme, explaining the lower K_d for ImC12. By contrast, the steric effect of an additional hydroxyl group in F87Y may

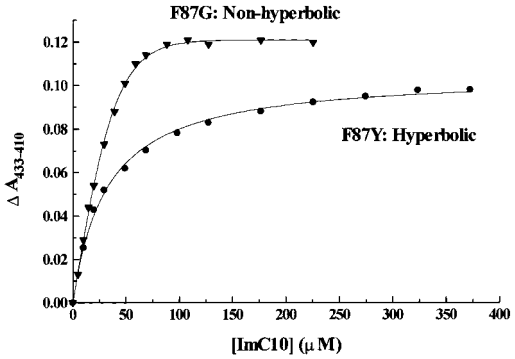

FIGURE 3: Overlay of the titration curves for the binding of ImC10 for site-directed mutants F87G (▼) and F87Y (●) of intact flavocytochrome P-450 BM3. Absorbance difference data were plotted vs [ImC10] as described in the Experimental Procedures section. The data for the F87G (3.1 μM) mutant titration are similar to those for the wild-type enzyme and reflect very tight binding ($K_d \leq 0.2$ μM). By contrast, ImC10 binds much more weakly to the F87Y mutant. The data for the F87Y mutant (3.5 μM) fit accurately to a rectangular hyperbola, giving a K_d of 32.2 μM.

restrict imidazole ligation to the heme, explaining the increased K_d (Table 3). The affinity of F87G for ImC10 was too high for a K_d to be determined accurately by spectrophotometric titration. However, the ImC10 titration curves for F87Y (even in the 1 cm path length cell) appear as perfect rectangular hyperbolae with a K_d value of 32.2 μM (Figure 3).

Residue W574 in the reductase domain of the flavocytochrome is conserved in eukaryotic P-450 reductases and is key to FMN binding, likely located directly above the isoalloxazine ring structure and providing aromatic stacking interactions that stabilize its binding to P-450 BM3 (*23*). Mutant W574D is essentially devoid of FMN (*18*). There is little alteration in the binding affinity of ImC12 to this mutant (7.7 μM) compared with the wild type (8.0 μM) (Table 3). Affinity for ImC10 remained very strong in W574D. Titrations of ImC10 and ImC12 were then performed with W574D saturated with 200 μM $NADP^+$. There was little effect on the affinity of ImC12 for $NADP^+$-saturated W574D compared with the $NADP^+$-free form (Table 3), and the nonhyperbolic trace for the ImC10 titration resembled almost exactly that for the $NADP^+$-free form at the same enzyme concentration (0.2 μM). These data indicate that $NADP^+$ binding does not affect significantly the affinity of the FMN-free enzyme for ImC12 (and probably not for ImC10 either).

Spectroscopic Characterization. CD spectra were run in the far UV region (190−260 nm) to assess whether the binding of the inhibitors (ImC10−ImC12 at 100 μM) induced detectable change in the secondary structure of P-450 BM3. However, the spectra were essentially identical ± inhibitors, indicating that inhibitor ligation does not induce gross changes in the protein structure. Resonance Raman (RR) spectra of inhibitor-bound (ImC10 and ImC12) and -free forms of the heme domain were then analyzed with excitation at 413.1 nm (Figure 4). This wavelength falls within the range of the Soret transition of the heme chromophore and produces Raman scattering from vibrational modes of the porphyrin ring. The resulting spectral bands are a probe of the conformation and the electronic structure of the heme, as well as oxidation and spin state of the iron center. The ImC10- and ImC12-bound forms are indistinguishable by

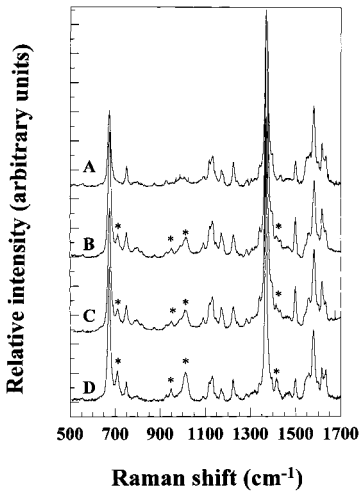

FIGURE 4: Resonance Raman spectra of the heme domain of flavocytochrome P-450 BM3 with Soret band excitation at 413.1 nm, as described in the Experimental Procedures section. (A) Oxidized ligand-free heme domain; (B) ImC10 complex; (C) ImC12 complex; (D) oxidized heme domain plus equivalent volume of solvent (DMSO/methanol 1:1 v/v) used for inhibitor addition in spectra B and C. The asterisk indicates peaks arising from the solvent.

RR spectra. However, differences are observed relative to the inhibitor-free form (Figure 4). The oxidation-state-sensitive band ν_4 is observed at 1371 cm^{-1} in all spectra, indicating that the iron center retains a ferric oxidation state upon inhibitor addition (24, 25). The spin-state sensitive bands ν_3, ν_{11}, ν_2, ν_{37}, ν_{38}, and ν_{10} display limited frequency differences, indicating that the iron has a low-spin electronic configuration in all the species (26). Differences are observed in the intensity of some bands. Most are in the 1450−1650 cm^{-1} frequency region. The stretching of the vinyl substituents and the breathing mode ν_3 of the porphyrin ring both become more intense upon inhibitor binding. Also, the band of the ring mode ν_{37} both decreases in intensity and shifts toward lower frequencies. The intensity of ν_{37} is affected by the orientation of the vinyl substituents relative to the porphyrin ring (27). Additional changes in intensity are observed for other bands in the 1100−1250 cm^{-1} region, namely ν_{44}, ν_{43}, and ν_{13}. These bands arise from modes including vibrations of both the vinyl substituents and the porphyrin ring (27).

Overall, the limited frequency shifts affecting ring vibrations suggest that no significant distortions in the structure of the porphyrin ring or in its core size occur on inhibitor ligation. This indicates that the ferric iron has not changed position relative to the porphyrin plane. However, it appears that the heme vinyl groups are reorientated on ligation of the azoles.

DISCUSSION

Pyridine and imidazole derivatives are particularly widespread as P-450 inhibitors. Derivatives that mimic aspects of the structure of the normal substrate for the P-450 targeted are generally the most effective inhibitors, since they combine the lipophilic nature and molecular geometry of the substrate with azole/pyridine functionality required to ligate the heme iron. Optimization of these features for the sterol 14α-demethylase P-450 from yeasts has led to the develop-

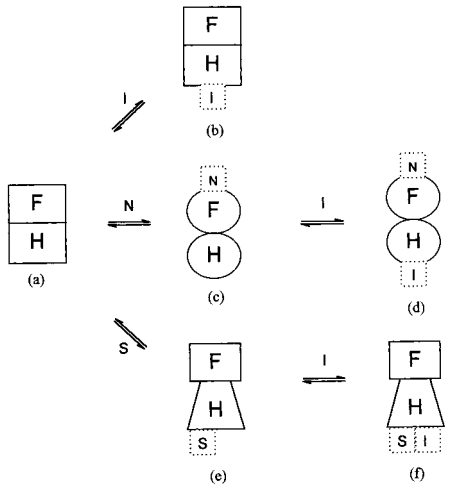

FIGURE 5: Schematic representation of the effect of association of substrates [$NADP^+$ (N) and fatty acids (S)] on the binding of imidazolyl carboxylic acid inhibitors (I) to the heme (H) of flavocytochrome P-450 BM3 (FH). The affinity of I for the substrate-free enzyme (a) is lower than that for the $NADP^+$-bound form of the protein (c), likely due to a favorable conformational change transmitted through the flavin domain (F) to the P-450. Affinity for I is also affected by the presence of fatty acid substrates (S), with a general increase in affinity with laurate-saturated enzyme and a decrease for the arachidonic acid-saturated form, presumably due to different binding mode-dependent conformational effects directly on the heme domain (e).

ment of effective antifungal agents such as ketoconazole, miconazole, and fluconazole (*12*). Similarly, metyrapone and its analogues have proved efficient inhibitors of the human 11β-hydroxylase enzyme that catalyzes the final step in the biosynthesis of cortisol, and these have been used in the treatment of hypercortisolism (Cushing's syndrome) (*28*).

The features of substrate-like structure and heme-coordinating azole group suggested that the imidazolyl carboxylic acids might be effective inhibitors of the P-450 BM3 fatty acid hydroxylase. This proved to be the case. The imidazolyl carboxylic acids (ImC10, ImC11, and ImC12) are potent reversible inhibitors at the heme site of P-450 BM3. They all show characteristics of mixed inhibition; i.e., they bind reversibly to both the free enzyme (E) and to the enzyme−fatty acid complex (ES) and have the apparent effect of increasing the K_m and decreasing the k_{cat} of P-450 BM3-catalyzed laurate hydroxylation. The parameters defining the relative potencies of the three inhibitors, K_{ic} and K_{iu}, the dissociation constants for their binding to E and to ES (Scheme 1), indicate that ImC10 is a more effective inhibitor (K_{ic} = 0.87 μM, K_{iu} = 5.70 μM) than either the ImC11 (K_{ic} = 7.5 μM, K_{iu} = 16.2 μM) or ImC12 (K_{ic} = 1.35 μM, K_{iu} = 6.94 μM).

Spectrophotometric studies of the binding of the inhibitors to the laurate- and arachidonate-saturated forms of P-450 BM3 proved that affinity for the inhibitors was retained, in agreement with the finding that all three behaved as mixed inhibitors. However, while arachidonate saturation diminishes inhibitor binding (elevated K_ds), laurate saturation enhances inhibitor binding (lower K_ds) in both P-450 BM3 and its heme domain (Tables 2 and 3). The results with laurate suggest that binding of this fatty acid may induce a conformational change in the active site of P-450 BM3 that allows enhanced binding of the inhibitors (Figure 5). It might be expected that binding of arachidonic acid (a superior substrate to laurate) would have an effect similar to that induced by laurate, substrate binding being known to cause considerable structural rearrangement in the P-450 BM3 active-site cleft (*7*). However, K_ds for the binding of ImC10−ImC12 to P-450 BM3 are increased with arachidonate. This likely reflects distinct modes of binding for these fatty acids; with the larger (C_{20}) polyunsaturated arachidonate protruding further down the active site and obscuring access to the heme, while the shorter (C_{12}) laurate adopts a conformation that not only permits co-binding of inhibitors but actually enhances their ligation. Additional experimental evidence for differential binding modes of distinct fatty acid substrates of P-450 BM3 also comes from other sources. For instance, resonance Raman studies indicate differing substrate-dependent effects on P-450 BM3 heme ring vibrations (29). Also, oxidation of arachidonic acid occurs with epoxidation to form 14,15-epoxyeicosatrienoic acid, reflecting the insertion of oxygen across a carbon−carbon double bond at positions ω-5 and ω-6 on the substrate, a position remote from the ω-1 to ω-3 favored for oxidation of saturated fatty acids (*9*, *30*). Previous studies have also indicated that co-binding of inhibitor/substrate can occur in P-450 BM3. For instance, the inhibitor metyrapone can bind simultaneously with palmitate (*31*). Co-binding of pyridine/laurate has also been observed by NMR (*32*). The co-binding of ImC10−ImC12 with fatty acids may be energetically favorable, with hydrophobic interactions between the molecules stabilizing their binding in the active site. However, the inhibitors must travel further into the active-site crevice of P-450 BM3 than do substrates, in order for their imidazole group to ligate the ferric iron (*7*, *32*, *33*). Thus, the dominant stabilizing interactions will be different for S and I in the ESI complex. The most important ES interaction will be between the fatty acid carboxylate and R47 (and possibly Y51), and for EI this will be between ferric iron and the imidazole group.

Pyridine dinucleotide binding also affects the affinity of P-450 BM3 for imidazolyl carboxylic acids, but by a different mechanism than that induced by bound fatty acid. Saturation with $NADP^+$ enhances binding of ImC11 and ImC12 (probably ImC10 also) to P-450 BM3 heme, presumably by transmission of a conformational change through the reductase domain (where the $NADP^+$ site is located) to the heme domain. The absence of such effects in FMN-free mutant W574D indicates that the effect involves this flavin cofactor. It is tempting to speculate that the binding of pyridine nucleotide induces structural realignment of the intact P-450 BM3 such that the reductase domain moves to interact with the heme domain and causes a structural change at the active site of the latter compatible with tighter binding of the imidazolyl carboxylates. This effect could be transmitted via bound pyridine nucleotide through FAD and FMN [which are likely to be closely spaced, assuming structural homology with the mammalian P-450 reductase (*34*)] and onto the heme via interaction at the distal face of the P-450 between the exposed edge of the FMN through the cysteine (C400) that ligates the heme iron. This effect cannot be transmitted in the absence of FMN. The interdomain effects induced by $NADP^+$ are consistent with the data of Murataliev and Feyereisen (*22*), who observed that fatty acid binding to P-450 BM3 induced flavin fluorescence in its reductase domain. Also, the fact that $NADP^+$ binding tightens the

ligation of the inhibitors helps to explain the differences observed between the K_d values from spectral titrations and the K_{ic} values from kinetic studies.

Studies of the binding characteristics of the inhibitors to R47 and F87 mutants of P-450 BM3 have confirmed the importance, suggested from crystallographic analysis, of these active-site residues in substrate/inhibitor interaction (*6*, *7*). The binding of ImC12 to the R47G mutant is characterized by a much higher K_d (42.2 μM) than that of the wild type (8.0 μM), a result consistent with a favorable charge−charge interaction between the positive guanidinium group of the R47 side chain and the negative carboxylate of ImC12. It is likely that the carboxylate group of ImC12 interacts with R47 in a fashion similar to that of substrates and that this is an important factor controlling association with the enzyme, prior to movement of the inhibitor further down into the active site for coordination to the heme iron. Residue R47 has a highly mobile side chain, and it has been proposed that substrate/R47 interactions are transient and that a hydrogen bond from residue Y51 is also important in protein−substrate carboxylate interaction (*7*). This provides a clear rationale for how both fatty acid and inhibitor can interact simultaneously with P-450 BM3. A binding "switch", whereby the substrate carboxylate moves from its electrostatic interaction with R47 to form a hydrogen bond with Y51, frees R47 to interact with the inhibitor carboxylate. After binding at the mouth of the active site, the inhibitor moves further into the channel to form the more stable imidazole/Fe^{3+} bond. This liberates R47, which can then share again with Y51 the role of stabilizing fatty acid binding to the oxidized P-450. Loss of this stabilizing effect in R47G results in a 5-fold decrease in affinity for ImC12. The importance of the R47−carboxylate interaction is also indicated by the recent demonstration of a large increase in the K_m for lauric acid with mutant R47E (which also showed enhanced binding of alkylammonium compounds) (*10*). The binding of ImC10 is also weakened in R47G, such that a K_d value (4.3 μM) can be determined in the 5 cm cell. This indicates that residue R47 is important for the binding of all the imidazolyl carboxylic acid inhibitors.

Mutant F87G shows slightly higher affinity for ImC12 than wild type (K_d = 5.3 μM), perhaps indicating improved access to the heme on removal of the aromatic side chain. The binding of ImC10 remains very tight with mutant F87G. By contrast, the affinity of ImC12 for mutant F87Y is decreased approximately 3-fold (K_d = 24.3 μM) from wild-type. The presence of the additional hydroxyl group may sterically impede ligation of this imidazole. Somewhat surprisingly, the affinity of F87Y for ImC10 is significantly decreased. The titration curve, even at 4 μM enzyme, is described accurately by a rectangular hyperbola, resembling those with ImC11 and ImC12. The K_d value obtained (32.2 μM) is similar to that for ImC12. These data confirm the critical role of F87 in controlling the active-site geometry and suggest that mutation F87Y causes a dramatic alteration of the heme environment. Other evidence from our studies on this mutant lead to the conclusion that significant active-site reorganization has occurred; specifically, that F87Y is insensitive to spin-state shift; showing <10% conversion to the high-spin form upon addition of up to 120 μM arachidonic acid (unpublished data). The data with mutant F87Y are consistent with a model in which the tighter binding of ImC10 can be explained in terms of its preferential association with a different conformer of the enzyme to that favored by ImC11/ImC12. Considerable conformational rearrangement occurs in the hydrophobic binding pocket on fatty acid binding as the heme iron is converted to the high-spin form (*7*). The conformer preferred by ImC10 may be one associated with the high-spin form of the enzyme; since binding of the substrate-like inhibitors may induce transient low- to high-spin conversion of the heme iron (prior to heme ligation) and since the binding of ImC10 is much weaker to the spin-state-insensitive F87Y.

All of the imidazolyl carboxylic acids bind to sodium dithionite-reduced P-450 BM3, but more weakly than to the oxidized form. However, they cannot ligate to fatty acid-saturated, reduced P-450 BM3. It is known that substrate binding induces major structural rearrangement in the active site (*7*), that the substrate binds initially to the P-450 at a distance (approximately 0.8 nm) too great for hydroxylation to occur (*7*, *12*), and that reduction of the heme iron facilitates movement of the substrate closer to the heme, brought about by conformational changes in the binding channel (*33*). It would appear to be the case that ImC10−ImC12 can access the heme in the oxidized, reduced, and oxidized/substrate-bound forms of P-450 BM3. However, in the reduced/substrate-bound form, the constriction of the binding channel and the close proximity of the fatty acid to the heme prevents ligation of the imidazole fatty acid. It is unlikely, therefore, that ImC10−ImC12 can inhibit P-450 BM3 efficiently at stages after the first electron transfer to the heme of the substrate-bound form.

In conclusion, we report here the identification of extremely potent inhibitors of the important flavocytochrome P-450 BM3 model system and characterize their inhibitory (K_i) and binding (K_d) properties. All are mixed inhibitors and ImC10 is the best-known inhibitor of P-450 BM3, with a K_d of <0.2 μM and K_{ic}/K_{iu} values of 0.87/5.7 μM. Use of ImC10−ImC12 as mechanistic probes has revealed a number of intriguing features. The inhibitors bind simultaneously with fatty acids and their binding strength is substrate-dependent. Lauric acid tightens considerably the inhibitors' affinity for ferric P-450 BM3. Residues R47 and F87 are important to inhibitor binding and the binding of ImC10, in particular, is dramatically weakened in the spin-state-insensitive mutant F87Y, suggesting that ImC10's high affinity may be for a specific conformer. Most importantly, the binding of $NADP^+$ on a distinct domain of P-450 BM3 tightens markedly the affinity for these heme-coordinating substrate analogues. The effect is not observed in a FMN-deficient mutant, indicating that this conformational effect is transmitted through the flavins. The imidazolyl carboxylic acid inhibitors are extremely useful probes of active-site geometry and interdomain effects and will prove important in future detailed analyses of mutant forms.

ACKNOWLEDGMENT

Imidazolyl fatty acids were provided by Ms. Ping Lu (Department of Medicinal Chemistry, University of Kansas).

REFERENCES

1. Lewis, D. F. V. (1996) in *Cytochromes P450: Structure, Function and Mechanism* pp 115−167, Taylor and Francis, London.

2. Munro, A. W., and Lindsay, J. G. (1996) *Mol. Microbiol. 20*, 1115−1125.
3. Park, S. Y., Shimizu, H., Adachi, S., Nakagawa, A., Izuka, T., & Shiro, Y. (1997) *Nat. Struct. Biol. 4*, 827−832.
4. Watanabe, I., Nara, F., & Serizawa, N. (1995) *Gene 163*, 81−85.
5. Marletta, M. A. (1993) *J. Biol. Chem. 268*, 12231−12234.
6. Ravichandran, K. G., Boddupalli, S. S., Hasemann, C. A., Peterson, J. A., & Deisenhofer, J. (1993) *Science 261*, 731−736.
7. Li, H.-Y., & Poulos, T. L. (1997) *Nat. Struct. Biol. 4*, 140−146.
8. Munro, A. W., Malarkey, K., Lindsay, J. G., Coggins, J. R., Price, N. C., Kelly, S. M., McKnight, J., Thomson, A. J., & Miles, J. S. (1994) *Biochem. J. 303*, 423−428.
9. Graham-Lorence, S., Truan, G., Peterson, J. A., Falck, J. R., Wei, S. Z., Helvig, C., & Capdevila, J. H. (1997) *J. Biol. Chem. 272*, 1127−1135.
10. Oliver, C. F., Modi, S., Sutcliffe, M. J., Primrose, W. U., Lian, L. Y., & Roberts, G. C. K. (1997) *Biochemistry 36*, 1567−1572.
11. Oliver, C. F., Modi, S., Sutcliffe, M. J., Primrose, W. U., Lian, L. Y., & Roberts, G. C. K. (1997) *Biochem. J. 327*, 537−544.
12. Schuster, I. (1993) *Medicinal Implications in Cytochrome P-450 Catalyzed Biotransformations* (Ruckpaul, K., & Rein, H., Eds.) Frontiers in Biotransformation, Vol. 8, pp 147−185, Akademie Verlag (VCH), Berlin.
13. Vanden-Bossche, H. (1992) *J. Steroid Biochem. Mol. Biol. 43*, 1003−1021.
14. Tuck, S. F., Peterson, J. A., & Ortiz de Montellano, P. R. (1992) *J. Biol. Chem. 267*, 5614−5620.
15. Lu, P., Alterman, M. A., Chaurasia, C. S., Bambal, R. B., & Hanzlik, R. P. (1997) *Arch. Biochem. Biophys. 337*, 1−7.
16. Miles, J. S., Munro, A. W., Rospendowski, B. N., Smith, W. E., McKnight, J., & Thomson, A. J. (1992) *Biochem. J. 288*, 503−509.
17. Munro, A. W., Daff, S., Coggins, J. R., Lindsay, J. G., & Chapman, S. K. (1996) *Eur. J. Biochem. 239*, 403−409.
18. Klein, M. L., & Fulco, A. J. (1993) *J. Biol. Chem. 268*, 7553−7561.
19. Daff, S. N., Chapman, S. K., Turner, K. L., Holt, R. A., Govindaraj, S., Poulos, T. L., & Munro, A. W. (1997) *Biochemistry 36*, 13816−13823.
20. Okita, R. T., Clark, J. E., Rice Okita, J., & Masters, B. S. S. (1991) *Methods Enzymol. 206*, 432−441.
21. Cornish-Bowden, A. (1996) in *Fundamentals of Enzyme Kinetics*, Portland Press, London.
22. Murataliev, M. B., & Feyereisen, R. (1996) *Biochemistry 35*, 15029−15037.
23. Porter, T. D. (1991) *Trends Biochem. Sci. 16*, 154−158.
24. Hildebrandt, P., & Stockburger, M. (1989) *Vibr. Spectrosc. Struct. 17*, 443−446.
25. Kitagawa, T., & Ozaki, Y. (1987) *Struct. Bonding 64*, 71−114.
26. Parthasarathi, N., Hansen, C., Yamaguchi, S., & Spiro, T. G. (1987) *J. Am. Chem. Soc. 109*, 3865−3871.
27. Choi, S., Spiro, T. G., Langry, K. C., & Smith, K. M. (1982) *J. Am. Chem. Soc. 104*, 4337−4344.
28. Ortiz de Montellano, P. R., & Correia, M. A. (1995) in *Cytochrome P450: Structure, Mechanism and Biochemistry* (Ortiz de Montellano, P. R., Ed.) pp 305−364, Plenum Press, New York.
29. Macdonald, I. D. G., Munro, A. W., & Smith, W. E. (1998) *Biophys. J. 74*, 3241−3249.
30. Miura, Y., & Fulco, A. J. (1975) *Biochim. Biophys. Acta 338*, 305−317.
31. Macdonald, I. D. G., Smith, W. E., & Munro, A. W. (1996) *FEBS Lett. 396*, 196−200.
32. Modi, S., Primrose, W. U., Boyle, J. M. B., Gibson, C. F., Lian, L. Y., & Roberts, G. C. K. (1995) *Biochem. J. 34*, 8982−8988.
33. Modi, S., Sutcliffe, M. J., Primrose, W. U., Lian, L. Y., & Roberts, G. C. K. (1996) *Nat. Struct. Biol. 3*, 414−417.
34. Wang, M., Roberts, D. L., Paschke, R., Shea, T. M., Masters, B. S. S., & Kim, J.-J. P. (1997) *Proc. Natl. Acad. Sci. U.S.A. 94*, 8411−8416.

BI980462D